Space-time influenza model with demographic, mobility, and vaccine parameters

E. Cahill, R. Crandall, L. Rude[1]

and

A. Sullivan[2]

19 Oct 05

Abstract: We present a space-time influenza model applicable to a large spatial region having variable population density. Spatial dependence is embodied in mobility effects (neighborhood diffusion and long-range travel), while temporal dependence arises from epidemic parameters and seasonal envelope. In discrete form, the model has been implemented to solve a nonlinear-diffusion system on each 10 km^2 pixel of a USA map. The model software implementation (URL download [8]) allows users to adjust a number of model parameters, including vaccination level in a given age group. We find that typical cumulative-case and mortality rates can be successfully modeled in stable fashion, in spite of the extensive, per-pixel computations. Moreover, our results on vaccination-mortality correlation are in essential agreement with previous works on smaller domains [32]. Our model should be deemed experimental, not as a policy generator itself but as a starting point for researchers, health workers, and policy makers interested in microscopic aspects of a national epidemic.

[1]Center for Advanced Computation, Reed College, Portland OR 97202
[2]Multnomah County Health Department, 426 SW Stark Street, 3rd Floor, Portland OR 97204

Background

Influenza has been a priority public health concern since it was identified as the cause of 1918's lethal pandemic. Avian flu circulating in Asia highlights our ongoing susceptibility to potentially pandemic strains, and recent disruptions in flu vaccine supply reveal vulnerabilities coping with a seasonal illness that kills an estimated 36,000 persons each year in the United States alone [29]. Policy makers need additional tools to assess the impact of influenza—whether an epidemic or pandemic strain. Here we present an extensively coupled space-time model appropriate for addressing questions of scale related to host and virulence factors for influenza.

Mass-action and mean-field models traditionally used by epidemiologist (see for example [1][2][17][22][24]) have been adapted in numerous ways to try to capture the spatial and temporal aspects of epidemic disease [13]. Some authors have used parameters to vary heterogeneity, mixing or variable population densities (e.g., [33]). Lattice models (e.g. [25]) more specifically address spatial issues by allowing interactions among neighboring cells in the lattice, including stochastic models where individuals interact on a Monte-Carlo basis (see [15][32]). Recent work on complex networks has emphasized the importance of stochasticity and spatial structure [31]. By exploiting recent advances in computing resources, such as the ability to involve many floating-point variables on each of many cells, we forge a hybrid approach to couple thousands to millions of quasi-autonomous populations that are specifically related through local, neighborhood, and long-distance travel parameters. This hybrid combines traditional mass-action principles with lattice and stochastic principles in a space-time model.

Our approach for a space-time influenza model describes annual scenarios for the United States of America (USA). We define this model—outlining our methods and underlying models—and describe the software (available at [8]) for its implementation. While we provide example results from software runs to demonstrate the utility of user's ability to vary parameters like age-specific vaccination prevalence, we encourage readers to run this software with their own scenarios of interest.

Methods and Results

Model assumptions

We start with the assumption of a stable population wherein at any time, t, the following subpopulations are represented:

- $S(t)$: Number of susceptibles.
- $I_i(t)$: Number of infecteds in one of two disease states, $i = 1, 2$.
- $R(t)$: Number of recovereds.
- $D(t)$: Number of dead.

This overall population is distributed with density $p(x, y)$ over a geographical domain $\mathcal{D}$. The domain $\mathcal{D}$ need not be connected (e.g., our implementation $\mathcal{D}$ includes Alaska and Hawaii). Stable density p is assumed, as we apply the model over one year on the notion that a single dominant influenza strain is in effect for that period in the United States (see [4] for dominant-strain rationale).

Every small land patch of 10 km^2 is given its own susceptible-infected-recovered SIR propagation system. An extensively coupled system is created in that the USA will consist of roughly 10^6 such patches that independently evolve in time—except for neighborhood and travel interactions, as below. A contracted SIR model is solved on *each* patch. The statistical character of real-world SIR propagation is embodied in parametric noise in that disease-coupling parameters are given a mean about which fluctuations are mandated. On issues of population and demographic data, see the discussion and references following our ultimate model equations (5.1). It is of interest that in this fashion we end up iterating several million space-time differential equations per week of epidemic. As a practical matter one such epidemic week requires a few seconds of CPU time on a modern PC.

Demographic age classes are taken into account. In our model, the classes, $\{i, c, m, o\}$, represent the following (interval notation $[x, y)$ here means $x \leq \text{age} < y$):

- infant i : age $\in [0.5, 5)$.
- child c : age $\in [5, 18)$.
- middle m : age $\in [18, 65)$.
- old o : age $\in [65, \infty)$.

When we refer to a space-time variable, say $S_A(x, y, t)$, the subscript A represents one of the age classes, i.e. $A \in \{i, c, m, o\}$. Thus, every 10 km^2 spatial land-patch has at any moment susceptibles S_A, infecteds I_A, recovereds R_A, and dead D_A.

The model is initialized to susceptible densities $S_A(x, y) = f_A p(x, y)$ on each land patch, where f_A is the demographic population fraction for each $A \in \{i, c, m, o\}$. The disease coupling parameter, β, represents person to person (i.e. intracell, or intrapixel if you will) infectivity of influenza and rate of contact among susceptibles and infecteds with homogenous mixing in each small land patch (pixel). Among infecteds, we initially assume two disease states, defined by infectivity of each state. Because the incubation period for influenza is short and persons can be infectious prior to symptom onset, no incubation period is specified. Rather disease state 1 is defined as early in disease when persons are most infectious; and disease state 2, later in infection when persons are less infectious. Coupling between infecteds and susceptibles is done through cross-age parameters delineating distinct combinations. For two, possibly distinct age classes $A, B \in \{i, c, m, o\}$ a parameter β_{AB} represents infection coupling between age classes A, B. For example, β_{io} is coupling for infants infected by old.

Human mobility across spatial patches is included through a tunable spatial-diffusion term. This term and the assumption of a spatially varying population density $p(x, y)$ induce spatial dependence in the model. A travel parameter specifically determines long-range infectious transfer. Region-dependent seasonal contours dynamically modify relevant model algebra as described below. The model assumes that there is an initial state with some disease and depicts a year-long epidemic.

The analysis to follow, though specially tailored for extensive computation, is based on known manipulations, starting from the pioneering [18] to modern method reviews such as [10]. We start from a spatially homogeneous, two-stage influenza model. For our initial model, we adopt the following time-independent variables indexed by disease states, k equal to 1 or 2:

- β_k: Disease coupling between susceptibles and infecteds for disease state k.
- γ_k: Rate of disease progression.
- μ_k: Mortality rate out of a given state.

Note that $1/\gamma_i$ is the mean time an individual spends in state i. Our simplified SIR-type model in the absence of vaccination is as follows:

$$\frac{dS}{dt} = -S(\beta_1 I_1 + \beta_2 I_2), \tag{3.1}$$

$$\frac{dI_1}{dt} = +S(\beta_1 I_1 + \beta_2 I_2) - \gamma_1 I_1 - \mu_1 I_1,$$

$$\frac{dI_2}{dt} = +\gamma_1 I_1 - \gamma_2 I_2 - \mu_2 I_2,$$
$$\frac{dR}{dt} = +\gamma_2 I_2,$$
$$\frac{dD}{dt} = +\mu_1 I_1 + \mu_2 I_2.$$

where we always have

$$\frac{d}{dt}\left(S + I_1 + I_2 + R + D\right) = 0,$$

with the total population conserved throughout time.

Model contraction

To cut down on computing resources—such as CPU and memory—we adopt a *one*-state model with renormalized parameters. Happily, proper renormalization yields approximate equivalence to the two-state model, as we shall see. From the third equation in system (3.1), we can define $I = I_1 + I_2$ and write

$$\frac{dI_2}{dt} = +\gamma_1 I - \Gamma I_2, \tag{3.2}$$

with a new parameter, $\Gamma = \gamma_1 + \gamma_2 + \mu_2$. The relation (3.2) may be integrated formally, to obtain

$$I_2(t) = \gamma_1 e^{-\Gamma t} \int_0^t e^{\Gamma \tau} I(\tau) d\tau,$$

on the presumption $I_2(0) = 0$. But this integral relation amounts to a so-called low-pass filter on the total infection I, i.e. an exponential weighting of $I(t)$ backward in time. We might therefore expect that for significant stretches of time we have

$$I_2 \approx \frac{\gamma_1}{\Gamma} I.$$

Given this approximation, it is generally possible to choose renormalized parameters for a one-state system to obtain very much the same time evolution for I as for the sum $I_1 + I_2$ in the original two-state system. Even when the integral approximation for I_2 is inexact, the overall dynamical trajectory of the sum $I_1(t) + I_2(t)$ can still be well approximated by choosing appropriate new parameters in a one-state system, with $I(t)$ being the approximating trajectory (Figure 1).

We subsequently adopt a suitably contracted, one-disease model system

$$\frac{dS}{dt} = -\beta S I, \tag{3.4}$$
$$\frac{dI}{dt} = +\beta S I - \gamma I - \mu I,$$
$$\frac{dR}{dt} = +\gamma I,$$

$$\frac{dD}{dt} = +\mu I.$$

While appearing to be a simpler SIR-type model, we are actually approximating our parameters in terms of the original, two-state-influenza parameters. With the use of Γ, the following additional parameter approximations ensue:

$$\beta = \beta_1 + \frac{\gamma_1}{\Gamma}(\beta_2 - \beta_1),$$
$$\gamma = \frac{\gamma_1\gamma_2}{\Gamma},$$
$$\mu = \mu_1 + \frac{\gamma_1}{\Gamma}(\mu_1 + \mu_2).$$

This one-state system (3.4) is viable for extensive computations on a great many spatial patches. There is the advantage that good stability is expected. For example, when including parametric noise (see below) an empirical two-state system is less stable than the one-state analogue, and that is a computational advantage for the one-state scenario.

For model-contraction with vaccination states, we include a population $V(t)$ of vaccinees. All vaccinations are *a priori*, so that the populations of susceptibles and of vaccinees at time $t = 0$ are

$$S(0) = (1 - v)\bar{S}(0),$$
$$V(0) = v\bar{S}(0),$$

where $\bar{S}(0)$ is the prevaccination susceptible population, and v is the fraction vaccinated. A suitable differential system is thus:

$$\frac{dS}{dt} = -\beta SI, \tag{3.5}$$
$$\frac{dV}{dt} = -\beta(1 - \theta)VI,$$
$$\frac{dI}{dt} = +\beta I(S + (1 - \theta)V) - \gamma I - \mu I,$$
$$\frac{dR}{dt} = +\gamma I,$$
$$\frac{dD}{dt} = +\mu I.$$

Vaccine efficacy, θ, and failure, $(1 - \theta)$, modify the intensity of disease transmission through a reduced likelihood of infection among vaccinees. The total susceptible, $\bar{S}$, is now defined to be $\bar{S} = S + V$. We then contract the model so that $\bar{S}$ is substituted for S, V by transforming the first three equations of (3.5) to the system,

$$\frac{d\bar{S}}{dt} = -\beta\bar{S}IJ,$$

$$\frac{dI}{dt} = +\beta \bar{S} I J - \gamma I - \mu I,$$

where

$$J = 1 - \theta \frac{V(t)}{\bar{S}(t)}.$$

Now, it may be derived that

$$J(t) = 1 - \theta v K(t),$$

where

$$K(t) = \frac{1}{1 - (1-v)(1 - (S(t)/S(0))^{\theta})}.$$

Note that $J(0) = 1 - \theta v$. For wide ranges of vaccination prevalence v and efficacy θ, the factor $K(t)$ is a function of only mild variation. For example, say that the disease is sufficiently aggressive that half of all nonvaccinated susceptibles become infected, so $S(\infty)/S(0) = 1/2$; and say that this occurs with efficacy $\theta = 0.75$ (or, if you will, 75%) and that a fraction $v = 0.5$ of the initial population is vaccinated. Then

$$J(0) = 1 - \theta v = 0.635, \;\; J(\infty) = 0.466,$$

As these extreme values do not differ significantly in magnitude, we simplify $J(t)$ to be a new, constant parameter, J, yielding the contracted model:

$$\frac{d\bar{S}}{dt} = -\beta(1 - \theta v)\bar{S} I, \tag{3.6}$$

$$\frac{dI}{dt} = -\beta(1 - \theta v)\bar{S} I - \gamma I - \mu I,$$

$$\frac{dR}{dt} = +\gamma I,$$

$$\frac{dD}{dt} = +\mu I,$$

which should be reasonably accurate, over a wide range of θ, v, in a sense similar to the effect shown in Figure 1 for $2 \rightarrow 1$-state contraction. Note that the first equation of (3.6) tells us that our new, collective-susceptible population $\bar{S}$ is given a lowered probability $1 - \theta v$ of infection, and it is this term that removes an explicit population V. This contraction is consistent with the notion that vaccination reduces the probability of infection approximately by a factor $(1 - \theta v)$. Clearly there are model simplifications of this type for time-varying v, θ, but because our USA Influenza model assumes vaccination takes place prior to the rapid rise of the influenza season, we shall take v_A, θ_A as constants, frozen at the first week of the time evolution.

Finally, because of demographic variation in both vaccination rates and effectiveness, prevalence of vaccination, v_A, and vaccine efficacy, θ_A, are both dependent on age class A.

Space-time model

Keeping the notion of a one-disease-state model, we now posit a space-time system including diffusion (mobility) and long-range travel of individuals:

- $S(x, y, t)$: Population density at spatial position (x, y), time t.
- $I(x, y, t)$: Infecteds density.
- β: Disease coupling involving local infecteds–susceptibles.
- β': Disease coupling from diffusion.
- T: Travel coefficient.

We say that $p(x, y)$ is the static population density at (x, y) for all S, I, R, and D, and that $\mathcal{D}$ is the geographical region within the USA over which the spatial integral of infecteds yields total infecteds at any given time.

A physically reasonable model is embodied in the following differential system:

$$\begin{aligned} \frac{\partial S}{\partial t} &= -S\left(\beta I + \beta' \nabla^2 I + Tp(x,y)\int_{\mathcal{D}} I\right), \qquad (4.1)\\ \frac{\partial I}{\partial t} &= +S\left(\beta I + \beta' \nabla^2 I + Tp(x,y)\int_{\mathcal{D}} I\right) - \gamma I - \mu I,\\ \frac{\partial R}{\partial t} &= +\gamma I,\\ \frac{\partial D}{\partial t} &= +\mu I. \end{aligned}$$

The quantity $p(x, y) = (S + I + R + D)(x, y, t)$ is conserved, i.e. time-independent by the usual argument that the right-hand-sides of (4.1) add to zero. This conservation law holds even though there is infection caused by long-range travel, summarized in the term

$$Tp(x, y)\int_{\mathcal{D}} I \; dx \; dy.$$

The integration over $dx \; dy$ is implicit in the display of (4.1). The term depends on how many infecteds there are nationwide, on the local population (on the assumption, e.g., that "small cities have small airports"), and on a travel "tendency" T.

This space-time model immediately yields observations of disease propagation. The second equation of the system (4.1), in *absence* of travel, say, $T = 0$, may be written

$$\frac{\partial I}{\partial t} = d\nabla^2 I + (\beta S - \gamma - \mu)I,$$

where $d := \beta' S$ is an instantaneous diffusion constant, so we have a kind of nonlinear diffusion equation. It turns out that there is a characteristic maximum propagation velocity (see [22] for a derivation) in a given locale (x, y):

$$u_{max} = \sqrt{4d(\beta S - \gamma - \mu)},$$

when the square-root exists, which formally it does if S is sufficiently large. An approximation for large susceptible population is

$$u_{max} \approx 2p(x, y)\sqrt{\beta\beta'}.$$

Thus, disease propagation into a small land patch with only susceptibles is proportional to the population density, and to the geometric mean of the static- and mobile-coupling parameters.

Discretization of the space-time model

The primary spatial-effects term in the system (4.1) is the diffusion piece $d\nabla^2 I$. This quantity can be given a discrete-lattice interpetation as follows. For a function $I(x, y)$ (time t is fixed here) defined on *pixel* positions (x, y) with unit spacing, it is a well known difference approximation that

$$\nabla^2 I \approx I(x+1, y) + I(x-1, y) + I(x, y+1) + I(x, y-1) - 4I(x, y),$$

which we write as

$$\nabla^2 I \approx -4I + \sum_o I,$$

where the sum is over orthogonal neighbors. Because the neighbor operations are not too computationally expensive, we adopt a more precise approximation

$$\nabla^2 I \approx -\frac{8}{3} I + \frac{1}{3} \sum{}' I,$$

where the $\sum'$ is now over all eight "king-move" neighboring values of I. This means that the discrete form of a relevant piece of the first equation in system (4.1) is

$$\beta I + \beta' \nabla^2 I \approx \beta_1 + \beta_2 \sum{}' I,$$

where

$$\beta_1 = \beta + 8\beta', \ \beta_2 = 3\beta'. \tag{4.2}$$

With this discretization rule, and using our previous simplified model equations, we now present a full, discrete space-time influenza model, this time moving directly to a scenario that includes vaccination and demographic groups.

In the following definitions, the subscripts 1,2 refer to the assignments (4.2), and we remind ourselves that subscripts $A, B \in \{i, c, m, o\}$ are age classes.

- $p(x,y) = p_i + p_c + p_m + p_o$: Stable population density at pixel (x,y), over domain $\mathcal{D}$.
- β_{1AB}: Static (local) infection coupling for infection $B \to A$.
- β_{2AB}: Mobile (neighboring) infection coupling for infection $B \to A$.
- $\theta_A \in [0,1]$: Vaccine efficacy parameter for age class A.
- $v_A \in [0,1]$: Vaccination prevalence of age class A.
- γ_A: Disease progression rate for age class A.
- μ_A: Mortality rate due to the disease, for age class A.
- T: Travel coefficient for long-range invasion of infecteds.
- $E(x,y,t)$: Overall seasonal-regional envelope.
- $\eta(x,y,t)$: A noise term recognizing erratic character of coupling.

Now the dynamical space-time variables are taken to be

- $S_A(x,y,t)$: Susceptible population of age class A at pixel (x,y).
- $I_A(x,y,t)$: Infecteds of age class A at pixel (x,y).
- $I(x,y,t) := I_i + I_c + I_m + I_o$: Total infecteds at pixel (x,y).
- $R_A(x,y,t)$: Recovereds of age class A at pixel (x,y).
- $D_A(x,y,t)$: Deaths in age class A at pixel (x,y).

Synthesizing all the previous ideas and methods, our influenza model system can now be displayed. There is one disease state, and no explicit vaccinated population tracked; instead, we use our previous conclusion that similar phase trajectories will accure for appropriate rescalings of key parameters. As usual, $A \in \{i,c,m,o\}$ denotes an age class. The change ΔX for any variable X will correspond to a one-week increment of time, with all β, γ, μ parameters appropriately normalized:

$$\Delta S_A = -S_A(1-\theta_A V_A)\left(\sum_B \beta_{1AB} I_B + \sum_B \beta_{2AB} {\sum_{\mathcal{D}}}' I_B + Tp(x,y)\sum_{\mathcal{D}} I\right)(1+\eta)E, \qquad (5.1)$$

$$\Delta I_A = -\Delta S_A - \gamma_A I_A - \mu_A I_A,$$

$$\Delta R_A = +\gamma_A I_A,$$

$$\Delta D_A = +\mu_A I_A.$$

Here, the total infected population is a discrete sum, $\sum_{\mathcal{D}}$, over all domain pixels. Note once again the sum of all four Δ-terms is zero, so that total pixel population $\sum_A (S_A + I_A + R_A + D_A)$ is invariant.

Nationwide effects include the seasonal envelope $E(x, y, t)$ which acknowledges seasonal differenes in disease coupling likely due to social and environmental effects. The baseline envelope function E is based on CDC national surveillance data [4]. In addition, during per-pixel computations, we consider travel invasion as a temporary fluctuation, so that over say a one-year influenza cycle the basic population $p(x, y)$ is stable, as determined by an initial population map.

Regarding the population-density data, U. S. Census data was used in a county-density mode [6] with the national demographic histogram [5] applied uniformly to each region. More precise, "pinpoint" densities for U. S. cities are available, (e.g., in [7]) but space-time modeling is problematic when sources are singular. Thus, we adopt county-specific census data, and use intrinsic noise in two ways. Our noise function ϵ (Table 1) allows us to start the space-time density $p(x, y, t)$ at time $t = 0$ as $p(x, y, 0) := p(x, y) \cdot (1 - \epsilon(x, y))$ such that a county has a slightly nonuniform density. A second noise function, η, is employed during temporal propagation of the model to avoid uniform evolution of all pixels in a region of uniform population density. To understand the importance of η, consider a large collection of land-patch pixels under a common seasonal/regional envelope with equivalent demographics and total population each. A deterministic differential or difference equation (say the first equation in 5.1 without the $(1 + \eta)$ term) would force all collected pixels to evolve in absolute unison. Such evolution would be unrealistic, and this synchrony could yield untoward resonance effects. To address this problem we use RMS noise that is essentially equivalent to fluctuations attendant on a truly discrete model of individuals. In our implementation, the RMS value $\sqrt{\langle \eta^2 \rangle}$ was set on the basis of numerical experiments over a moderately populated collection of pixels whose individuals sustain an epidemic in probabilistic fashion. Ultimately, each of our 10 km^2 pixels in a given county starts with a nonuniform population, and as the difference equations propagate disease, like pixels behave slightly differently.

In our model (5.1), β_{jAB} for $j = 1, 2$ is the infection coupling for a $B \to A$ infection. We specify matrices of such β parameters in the form:

$$\{\beta_{1AB}\} = \beta_1 \begin{pmatrix} \rho\sigma & \rho\sigma & \sigma & \sigma \\ \rho\tau & \rho\tau & \tau & \tau \\ \rho & \rho & 1 & 1 \\ \rho & \rho & 1 & 1 \end{pmatrix}, \tag{5.2}$$

$$\{\beta_{2AB}\} = \beta_2 \begin{pmatrix} \sigma & \sigma & \sigma & \sigma \\ \tau & \tau & \tau & \tau \\ 1 & 1 & 1 & 1 \\ 1 & 1 & 1 & 1 \end{pmatrix}.$$

Here, the first row of a matrix corresponds to fixed $A = i$ and ranging $B \in \{i, c, m, o\}$. Thus, model (5.1) as intended for implementation involves five coupling parameters, $\beta_1, \beta_2, \rho, \sigma, \tau$.. The three parameters ρ, σ, τ can be used to amplify disease coupling by age class, subsequently affecting infection acquisition in certain age classes (e.g., i, c) and the infection threat of one class on another.

Software implementation

We implemented the system (5.1) as USAFluModel v1.4 [8], on Mac OS X v. 10.3x. The discrete space-time model is solved on every pixel independently, except of course for the nighbor terms $\sum_k I$ and the travel invasion term proportional to T. With 1 GHz. processor, one week of influenza propagation across the full USA domain requires a few seconds of CPU; the full year, a few minutes of CPU.

Baseline influenza parameters used are directly from or calibrated to those defined by Weycker, et al. [32] (Table 1). After initialization, one is free to adjust the parameters in the parameter panel (Figure 3). Once parameters have been set the model can then be run, always starting in a week in October of any year, with the disease progression modeled via pixel coloring. Loosely speaking—for we do amplify certain colors for visual convenience—the colorings are:

- The *green* pixel channel is proportional to remaining susceptibles $(S_i + S_c + S_m + S_o)$.
- The *red* pixel channel is proportional to infecteds $(I_i + I_c + I_m + I_o)$.
- The *blue* pixel channel is proportional to recoverds $(R_i + R_c + R_m + R_o)$.

Results from software runs

We report herein influenza-related mortality under four scenarios: an average influenza year in the United States based on 1990 through 2003 flu seasons; an otherwise average year from this period in which a higher then average number of children are vaccinated; an otherwise average year from this period in which long-distance coupling is decreased; and an otherwise average year from this period in which neighborhood coupling is decreased.

In an average flu year based on default parameters for our first scenario, cumulative influenza cases numbered about 32,000,000, while total deaths numbered about 36,000 (Table 2). Increasing the prevalence of children vaccinated (age classes i, c) reduce morbidity and mortality; and the more children and infants vaccinated, the greater the effect. Reduced long-range travel slightly lowers total cases and deaths. However, reduced neighborhood coupling results in case and death totals that are roughly 40 percent below the values resulting for the default parameters. Only a very high prevalence of vaccination in age classes i and c has a greater effect on morbidity and mortality.

The pattern of morbidity seen across the U.S. reflects that the total numbers are not the whole picture. Mid-way through flu season, a patchwork of heavily infected regions and smaller pockets illustrate distinctly local impacts (Figure 4). Toward the end of a one-year cycle, recovereds dominate nationwide (Figure 4). The software allows manual blow-up of any region, and after a whole year's run, results are reported (Figure 5).

Discussion

The space-time model and concurrently developed software described here will hopefully aid policy makers in their understanding of the annual influenza epidemic. (For some discliamers, see the remarks at the end of this section.) Power for the end-user comes from control over a number of model parameters, allowing the exploration of multiple possible outcomes. The computational issues addressed in our approach highlight a balance between the intracacy and exactness of more epidemiologically detailed models with contractions and simplified disease assumptions to allow for computational complexity ([13]). While we rely on real-world data to establish baseline parameter values, the power of this model comes from the patterns evolved through computational effort—not from detailed estimates of incompletely defined quantities like transmissibility.

Regarding the specific findings of our model, our first scenario was used to define fixed parameters, and as such would obviously match known estimates of influenza mortality. The related rates of morbidity are difficult to verify, as influenza is not a nationally notifiable condition. However, given an estimated 200,000 influenza-related hospitalizations each year [3][29], it is reasonable to expect another 100-200 community cases of more mild illness for each hospitalization [19]. Also, our morbidity estimate for all cases is within the range of other similarly broad estimates [21]. In our second scenario, wherein the prevalence of vaccinated children is increased, we find reasonable agreement with other models, notably that of Weycker, et al. [32]. These consistencies give us confidence about the behavior of our model and the results of our other scenario. Given the relationship of the beta parameters, the large impact of reduced neighborhood coupling is difficult to interpret. However, if one can assume that certain unspecified biological aspects of β are consistent within age class for the major influenza strain in a given year, much of the effect of adjusting neighborhood coupling can be attributed to factors impacting the likelihood of contact between infecteds and susceptibles. These factors could include public health interventions like isolating ill persons at home or decreasing interactions among people in any location like work, school, or perhaps nursing homes.

As inferred above, one of the key simplifications in this model relates to the development of the set of β parameters. These disease coupling parameters represent potentially complex micro-level interactions. Contributors to disease coupling include the average likelihood of infection given exposure to an agent, and the likelihood of the exposure itself. The former is complicated by the proximity and duration of exposure; the latter, by the need to address coupling both within and among domains. The sheer complexity of these issues—both theoretical and computational—necessitated the use of a *de facto* set of β's in this current

version of the software. The parameter values applied were based on relationships among available pieces of real-world data. However, a remaining challange to address in future models of this lineage is to break up β into component parts. Not only would this next step provide parameters that can be more directly adjusted and more readily interpreted, but it would also help in evaluating the accuracy of the current values. For example, if the current values derived were consistent with reproductive ratios (R_0's) on the order of 1's to 10's, we would appear to have developed a reasonable estimate; if they were consistent with R_0's on the order of 100's or 1000's we would need to seriously reexamine our assumptions [20] [14] [28] [26] [12].

We make assumptions in the stability of our population. First, by excluding birth and death rates, we are assuming a stable, closed population for the course of the year in which the model is run. We also assume a degee of stability in underlying demographic information between census periods. Both of these assumptions are reasonable at the national level, though there may be localities where such assumptions are invalid. We simplified the notion of spatial population density to reduce considerable computations in several ways, with noise functions acting as best estimates on expected fluctuations. Along these lines, we acknowledge that certain local community or cultural effects—such as school crowding, etc.—are absent from the model. Noise effects and variable disease coupling make local variations implicit in the model, and allow for useful, *scaled* results at the national level. Naturally, more refined models can go a long way in lifting these simplifications, though at the cost of deeper computation.

The model contraction itself also yields a number of interesting observations. One important conclusion is that the new, single-disease-state parameter γ is a perturbed-half-harmonic mean of γ_1, γ_2. That is, for small μ_2 one has $1/\gamma \approx 1/\gamma_1 + 1/\gamma_2$, as in the combination of parallel resistors in electronic networks. In this way the model (3.4) is taking into account the *harmonic* addition of disease progression rates, in order to allow—to a good approximation—the contraction to just one disease state (one variable, $I(t)$). Along these lines, the system (3.4) was adopted for the time-dependent portion of our software implementation, with certain CPU, memory, precision, and stability advantages. For example, certain parameters are allowed to drift, or possess noise, but the basic structure of the time-dependent system remains that of (3.4). Just as a 2-disease-state model can be contracted to an approximately equivalent 1-disease-state model (provided the disease progression and mortality parameters are suitably rescaled), a vaccination model can be contracted by rescaling the infection coupling β to be vaccine-dependent, i.e. to involve just one susceptible state that effectively contains the vaccinateds. Based on our numerical experiments, other complications (more than two disease states, vaccinated infecteds having a distinct disease coupling back to susceptibles, etc.) can usually be contracted.

It is also worth noting that disease propagation speed into a purely susceptible region is proportional to the population density, and to the geometric mean of the static- and mobile-coupling parameters. There exists theories of "epizootic waves," mainly for mammals such as rabid foxes [22]. We are not saying that influenza epidemics will appear as mixed, explicit waves, but it is valuable to keep in mind that in any suitable space-time model, the disease

should not propagate faster than a certain limit such as u_{max}. The telling fact is, once both space and time are involved in any model, there must always be a way to combine parameters to get entities of physical dimension length/time. Our maximum speed u_{max} is one such entity. Indeed, letting the symbol L denote length, and T time, we have physical dimensions:

$$\beta : L^2/T; \quad \beta' : L^4/T,$$

where both of these can be gleaned from the differential form (4.1), recalling that S, I are each densities and so have dimension L^{-2}. Being as $p(x, y, t)$ has dimension L^{-2} also, we find sure enough: the dimension of u_{max} is L/T, as a speed always must be.

As with all epidemiologic mass-action models, the power of this model also derives from its organization of theory into context for host/pathogen interactions, not in providing exact predictions of what will be. Thus, we do not assume that our discrete space-time model as implemented would be predictive on any absolute measure, such as infant (ages 0-5) mortality. Rather, we do expect useful results on questions such as "What is the approximate *fractional* decrease in deaths if vaccination prevalence is doubled for each age group?" Or: "What is the effect of vaccinating all children over 6 months old?" We could in future work also seek to include adjustable variables for the impact of use of antivirals as a measure to combat the affects of flu. We expect that modeling year-to-year variations of a recurring epidemic should be possible, yet more research is needed to include emergent mutants, use of neurominidase inhibitors, and nonrespiratory spread as with avian influenza viruses. Finally, another area for future research is to install into the model some knowledge of scale-free networks. Other attempts at epidemic modeling are quite complementary to ours in this respect: By focusing on contact logic, social networking, and so on to determine epidemic potential we can provide a more complete picture of our human condition.

Another interesting direction for future research is to model yet more microscopically. Our present software implementation shows that it is possible to model an entire nation on a per-pixel basis. But computational resources have reached the point where finer population density data and regional dependence of demographics should be within reach. In fact, the whole issue of population density as it appears in the governing equations is profound. For one thing, we have yet no satisfactory theory of the interplay between population density and the neighborhood diffusion parameter.

We close with some appropriate scientific disclaimers. This model—together with its software implementation [8]—should be taken as *experimental*. That is, knowing how delicate health-policy issues can be—especially for a large population—we present this model in the following spirit: We are endeavoring to answer the question "How can a national model be constructed with sufficient attention to the microscopic aspects?" Thus, our model stands as a kind of conceptual complement to, say, a classical SIR model (with just a few variables for one gigantic, national cell) over one influenza season. Along such lines, various issues have been pointed out to us authors—such as whether it would be better to model everything in discrete, cellular-automaton (CA) fashion and not to mix mean-field and diffusion models, as we have done; or whether to refine even further the coupling matrix $\{\beta_{1AB}\}$ including possible spatial

sensitivity; or how to render the travel term with more attention to geographical concerns, such as urban/suburban mobility, and so on. We take it as promising that our vaccine-induced mortality reductions are in essential agreement with other works on smaller spatial domains ([32]); yet again, we stress that our model should not itself dictate policy, but should open up research dialogue on how we might model microscopically a national epidemic.

Acknowledgements

We thank G. Crandall for software engineering, G. Oxman, B. McPhail for research and advice on epidemics in general, and S. Wolfram for feedback on the manuscript. M, Elman provided an excellent critical reading of the manuscript. A. Dworkin and E. Landhuis have been curious and encouraging voices from the media sector.

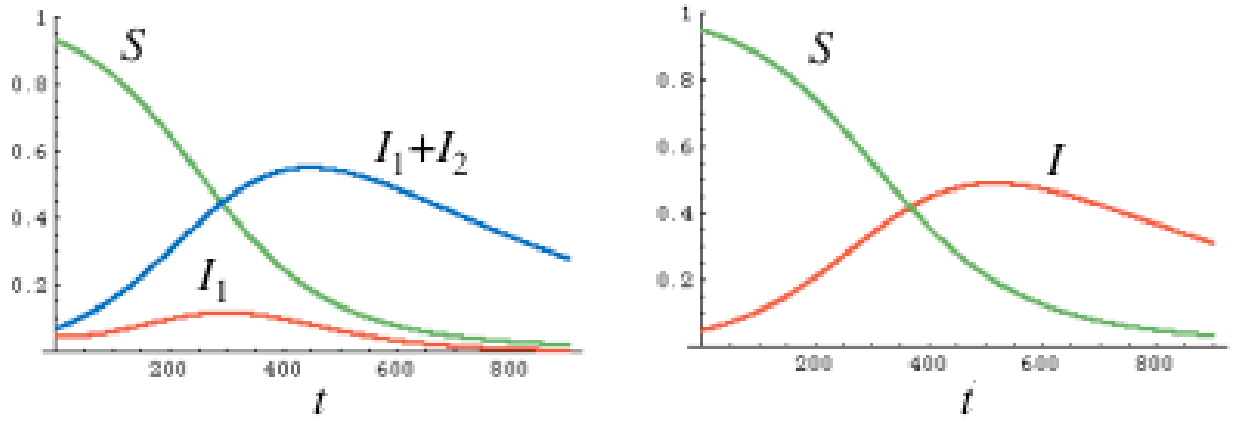

Figure 1: The concept of model contraction. The left-hand plot is for a typical manifestation of system (3.1), and so with two infectious densities I_1, I_2. The right-hand plot is of a *one*-state system with essentially equivalent behavior because of rescaled parameters, as in the contracted system (3.4). Similar contraction is possible for vaccination states, as in the contracted model (3.6).

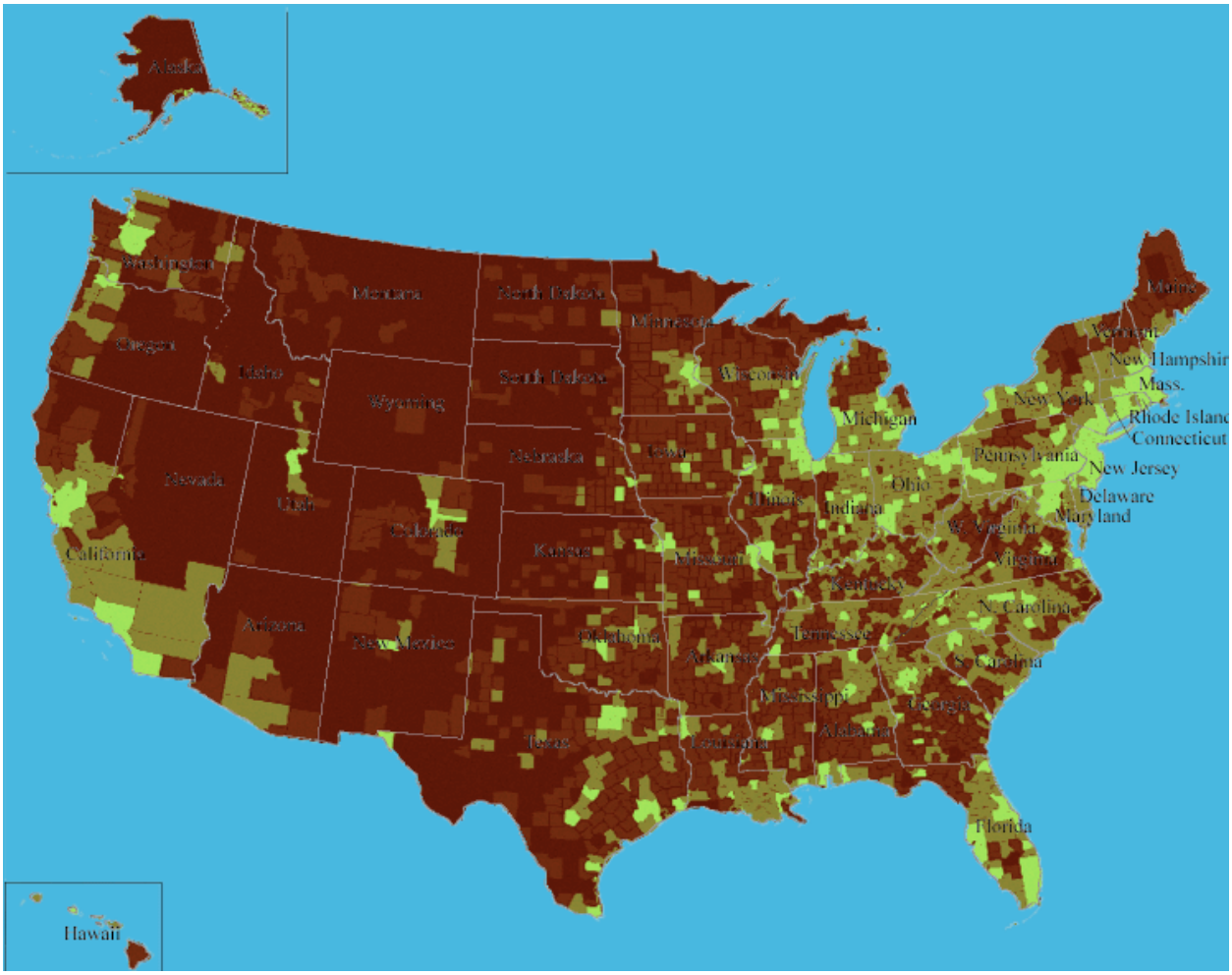

Figure 2: The initialization map, setting per-pixel population $p(x, y)$. Some initial infection is posited according to density statistics.

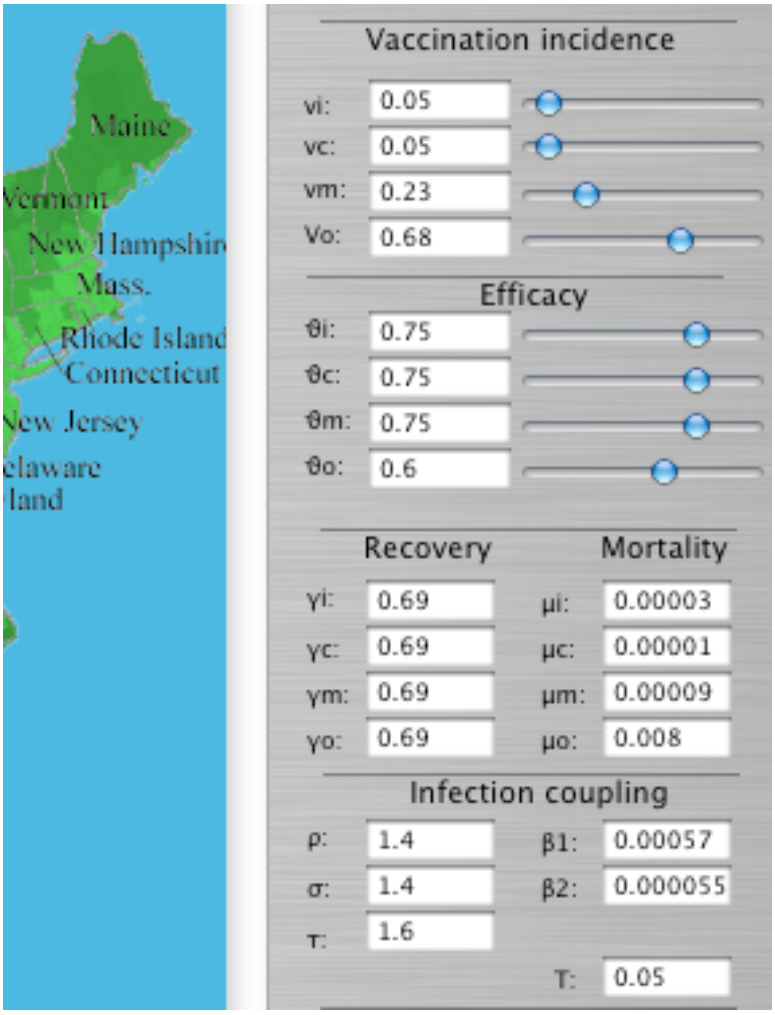

Figure 3: The parameter panel, showing default values pertinent to the known influenza statistics of 2003.

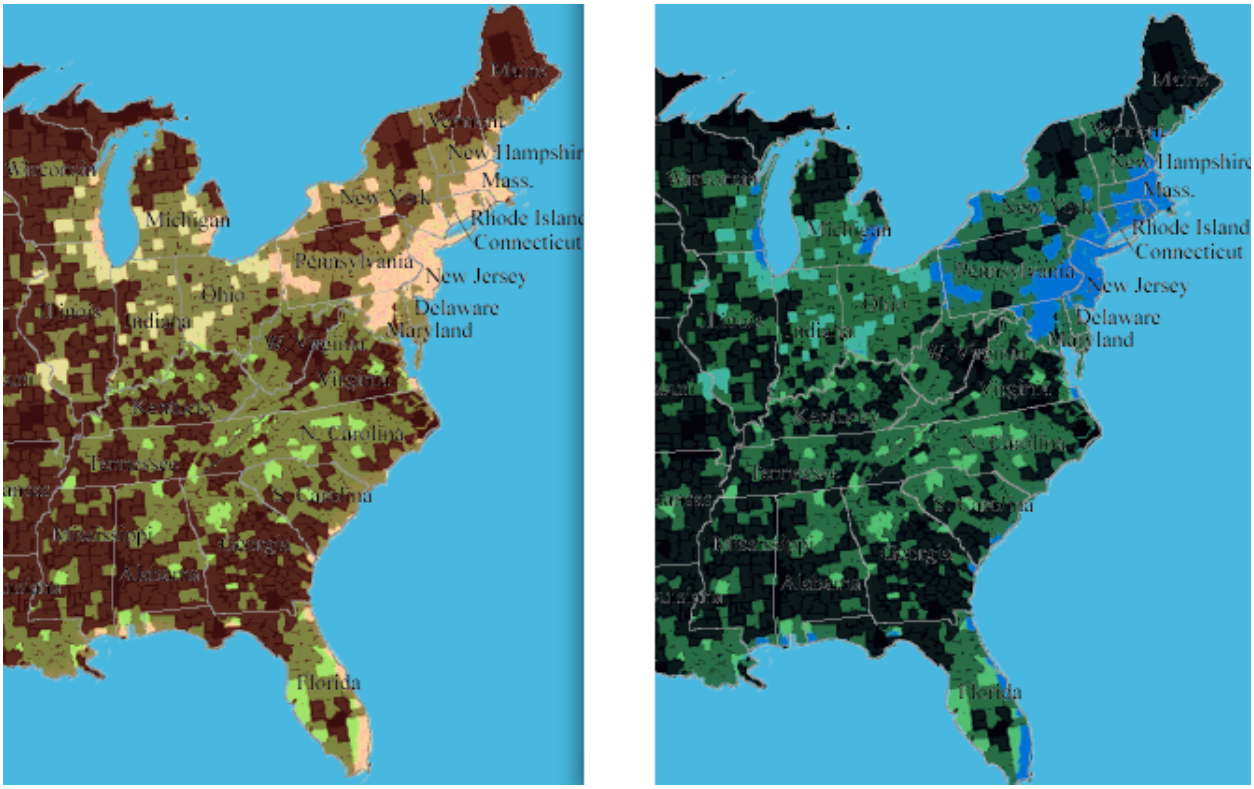

Figure 4: The Eastern seaboard in mid-February (left) with the given default parameters. There are some low-infection (green or light green), moderate infection (yellow pixels), and heavy infection (reddish) areas. Later, in August (right) areas of recovery (bluish land pixels) are evident (see also Figure 5).

Figure 5: The Oregon–Washington region in May, showing areas of recovery (bluish), and a sheen of underlying noise effects (i.e., colors are not entirely uniform across regions).

Infections:	85
Cumulative:	30830080
Deaths	
i:	611
m:	425
o:	33653
Total:	34689

Figure 6: The software reports, for the default pameters, some 30 million cumulative cases, and some 30 thousand deaths, showing age-class deaths in detail.

Parameter	Default value	Comments
$p_A(x,y)$	—	Spatial density from Census data [5][6]
β_1	0.00057	Local-infection (o,o) coupling
β_2	0.000055	Neighborhood (o,o) coupling
ρ	1.4	Multiplier for i,c infecteds (equ. (5.2) and [32])
σ	1.4	Multiplier for i susceptibles (equ. (5.2) and [32])
τ	1.6	Multiplier for c susceptibles (equ. (5.2) and [32])
θ_A	$\{0.75, 0.75, 0.75, 0.6\}$	Vaccine efficacy, age classes $A \in \{i,c,m,o\}$
v_A	$\{0.05, 0.05, 0.23, 0.68\}$	Vaccination incidence, $A \in \{i,c,m,o\}$
γ_A	$\{0.69, 0.69, 0.69, 0.69\}$	Disease progression rate, $A \in \{i,c,m,o\}$ [32]
μ_A	$\{3,1,9,800\} \cdot 10^{-5}$	Mortality rate, $A \in \{i,c,m,o\}$
T	0.05	Travel coefficient
$E(x,y,t)$	$---$	Seasonal envelope function, [4]
$\sqrt{\langle \eta^2 \rangle}$	0.07	RMS noise value (see text after (5.1))
$\sqrt{\langle \epsilon^2 \rangle}$	0.05	RMS noise value (see text after (5.1))

Table 1: Default parameters for the model (5.1). Except for population density p_A, seasonal envelope E, and RMS noise figures for η, ϵ all parameters are user-adjustable, as in Figure 3. Note that, via our matrix relation (5.2), all possible disease couplings are determined by parameters $\beta_1, \beta_2, \rho, \sigma, \tau$. All rate parameters assume a time differential of one week. For example, μ_A has units of individual risk per week. Our default values follow when possible the data given in the recent treatment [32].

Run	v_i	v_c	T	β_2	Cases	Deaths
Default run	D	D	D	D	32100000	36200
Increased infant-child vaccination	0.20	0.20	D	D	23800000	26200
Increased infant-child vaccination	0.50	0.50	D	D	7860000	8810
Reduced travel	D	D	0.016	D	30500000	34800
Reduced neighborhood coupling	D	D	D	0.000044	18800000	20500

Table 2: Results of running USAfluModel 1.4 [8] for one year, with certain specified adjustments (D = default value from Table 1). Mean values of cases and deaths over 15 runs for each table row. Standard deviations are nonzero across runs, because the model does have a stochastic component to avoid false synchrony. Deviations for reported cases/deaths are all found to be in the region of 0.5%, so the reporting here is done to three significant figures only.

References

[1] R. Anderson and R. May, "Population biology of infectious diseases 1," *Nature* 280:361 (1979).

[2] R. Anderson and R. May, *Infectious diseases of humans: Dynamics and control*, Oxford University Press, 1991.

[3] WM Barker. "Excess pneumonia and influenza associated hospitalization during influenza epidemics in the United States, 1970-78" *American Journal of Public Health*, 76(7):761-5 (1986).

[4] Center for Disease Control, regional boundaries and seasonal contours, at

`http://www.cdc.gov` (2004).

[5] US Census Bureau, "Profile of general demographic characteristics" and USpopulation.xls,

`http://www.census.gov/Press-Release/www/2001/demoprofile.html`, (2001, 2004).

[6] US Census Bureau, "U.S. population Density by Counties,"

`http://www.census.gov/dmd/www/pdf/512popdn.pdf`, (2001, 2004).

[7] US Census Bureau, "2000 U.S. population density,"

`http://www.census.gov/geo/www/mapGallery/2kpopden.html`, (2000).

[8] G. Crandall and R. Crandall, USAfluModel v1.4,

`http://academic.reed.edu/epi` (2005).

[9] C. Dibble and P. Feldman, "The GeoGraph 3D Computational Laboratory: Network and Terrain Landscapes for RePast," *Journal of Artificial Societies and Social Simulation*, 7:1,

`http://jasss.soc.surrey.ac.uk/7/1/7.html` (2004).

[10] O. Diekmann and J. Heesterbeek, *Mathematical epidemiology of infectious diseases*, John Wiley and Son (2000)

[11] R. Durrett and S. Levin, "The importance of being discrete (and spatial)," *Theoretical population biology*, 46:363-394 (1994).

[12] Fraser, C., Riley, S., Anderson, R.M. and Ferguson, N.M., "Factors that make an infectious disease outbreak controllable," Proc. Natl Acad. Sci. USA 101, 6146–6151 (2004).

[13] MN Ferguson, MJ Keeling, WJ Edmunds, R Gani, BT Grenfell, RM Anderson, and S Leach, "Planning for smallpox outbreaks," *Nature*, 425:681-685 (2003).

[14] Gog, J.R., Rimmelzwaan, G.F., Osterhaus, A.D. and Grenfell, B. T., "Population dynamics of rapid fixation in cytotoxic T lymphocyte escape mutants of influenza," A. Proc. Natl Acad. Sci. USA 100, 11143–11147 (2003).

[15] M. Halloran, I. Longini, A. Nizam, and Y. Yang, "Online supporting documentation: Can we contain bioterrorist smallpox?," manuscript (2002).

[16] U.S. National Center for Health Statistics, *National Vital Statistics Report (NSVR)*, 2004.

[17] E. Holmes, "Basic epidemiological concepts in a spatial context," in *Spatial ecology: The role of space in population dynamics and interspecific interactions*, D Tilman and P. Kareiva eds., Princeton University Press (1997).

[18] W. Kermack and A. McKendrick, "A contribution ti the mathematical theory of epidemics," *Proc. Roy. Soc,. London*, 115:700-721 (1927).

[19] P Lewis. Personal communication regarding electronic surveillance data for influenza-like illness (2005).

[20] Longini, I. M. Jr, Halloran, M. E., Nizam, A. and Yang, Y., "Containing pandemic influenza with antiviral agents," Am. J. Epidemiol. 159, 623–633 (2004).

[21] MI Meltzer, NJ Cox, and K Fukuda, *EID*, 5(5):659-71 (1999).

[22] J. Murray, *Mathematical biology*, Springer–Verlag (1989).

[23] US Public Health Service, "Vital Statistics of the United States, annual," Vols. I and II, 1900-1970.

[24] C. Rhodes and R. Anderson, "Power laws governing epidemics in isoplated populations, *Nature*, 381, 600-602 (1996).

[25] C. Rhodes and R. Anderson, "Epidemic Thresholds and Vaccination in a Lattice Model of Disease Spread," *Theoretical population bioloy*, 52:101-118 (1997).

[26] Rvachev, L.A. and Longini, I.M. Jr, "A mathematical model for the global spread of influenza," Math. Biosci 75, 3-22 (1985).

[27] R. Schinazi, "On the role of social clusters in the transmission of infectious diseases," *Theoretical population biology*, 61:163-169 (2002).

[28] Spicer, C. C. and Lawrence, C.J., "Epidemic influenza in Greater London," J. Hyg. (Lond.) 93, 105-112 (1984).

[29] W. Thompson, et al., "Mortality associated with influenza and respiratory syncytial virus in the Unites States," *JAMA*, 289, 2001, 179-186.

[30] J. van den Berg et al., "Dependent random graphs and spatial epidemics," *Annals of Applied Probability*, 8:317-336 (1998)

[31] J.A. Verdasca et al., "Recurrent epidemics in small world networks,".

[32] D. Weycker, J. Edelsberg, M. Halloran, I. Longini Jr., A. Nizham, V. Ciurlyla, G. Oster, "Population-wide benefits of routine vaccination of children against influenza," *J. Vacc.*, 4828-1-10, 2004.

[33] JA Yorke, HW Hethcote, and A Nold, "Dynamics and control of the transmission of gonorrhea," *Sex Transm Dis*, 5:51-56 (1978).